Flow Turbulence Combust
DOI 10.1007/s10494-010-9322-z

Large Scale Accumulation Patterns of Inertial Particles in Wall-Bounded Turbulent Flow

Gaetano Sardina · Francesco Picano · Philipp Schlatter · Luca Brandt · Carlo Massimo Casciola

Received: 16 December 2009 / Accepted: 15 December 2010

Abstract Turbulent internal flow in channel and pipe geometry with a diluted second phase of inertial particles is studied numerically. Direct numerical simulations (DNS) are performed at moderate Reynolds number ($Re_\tau \approx 200$) in pipe and two channels—a smaller one similar in size to previous studies and a 3×3-times larger one—and Eulerian statistics pertaining to the particle concentration are evaluated. This simulation box constitutes the largest domain used for particle-laden flows so far. The resulting two-point correlations of the particle concentration show that in the smaller channel the particles organize in thin, streamwise elongated patterns which are very regular and long. The spanwise spacing of these structures is 120 and 160 plus units for the channel and pipe, respectively. Only in the larger box, the streamwise extent is long enough for the particle streaks to decorrelate, thus allowing the particles to move more freely. The influence of the box size on the characteristics of the turbophoresis is clearly shown; a 10% increase of the near-wall correlation is observed for particles with Stokes number $St^+ = 50$. It is thus shown that the box dimensions are an important factor in correctly assessing the motion of inertial particles, and their relation to the underlying velocity field. In addition the binning size effects on the correlation statistics of particle concentration are exploited. In particular the spanwise correlation peak values appear very sensitive to the adopted binning size, although the position of these peaks is found almost independent. Hence to allow a significant comparison between data of different configurations it is necessary to adopt the same binning spacing in inner variable.

G. Sardina (✉) · F. Picano · C. M. Casciola
Dipartimento di Ingegneria Meccanica e Aerospaziale, Sapienza University of Rome,
via Eudossiana 18, 00184 Rome, Italy
e-mail: gaetano.sardina@uniroma1.it

P. Schlatter · L. Brandt
Linné Flow Centre, KTH Mechanics, Osquars backe 18, 100 44 Stockholm, Sweden

P. Schlatter
e-mail: pschlatt@mech.kth.se

Published online: 11 January 2011

Keywords Particle laden flows · Wall bounded flows · Turbophoresis · DNS · Turbulence · Inertial particles

1 Introduction

The dynamics of small inertial particles transported by a turbulent flow is crucial in many engineering applications. For instance internal combustion engines or rockets involve the interaction between small droplets, chemical kinetics and turbulence.

Small, diluted particles, much heavier than the carrier fluid, are essentially forced only by the viscous drag. Hence their velocity v is determined by $\dot{v} = (u - v)/\tau_p$, where $\tau_p = d_p^2 \rho_p / (18 \rho \nu)$ is the Stokes response time (d_p, ρ_p are the particle diameter and density respectively; ρ and ν are the fluid density and viscosity). In this model Lagrangian fluid particles are recovered in the limit of vanishing Stokes time. The opposite limit of ballistic particles is achieved for τ_p tending to infinity. The difference between particle velocity v and fluid velocity u produces various anomalous phenomena such as small-scale clustering or preferential accumulation at the wall (turbophoresis) even for incompressible flows, see among others [1–4].

Inertial particles in turbulent wall-bounded flow are characterized by the so-called turbophoresis phenomena, i.e. preferential accumulation close to the wall. Under appropriate conditions, particles may achieve extremely large concentrations at the wall, up to thousand times the mean value. This turbulence-induced transport and the issuing preferential accumulation has been addressed in a number of papers dealing with a variety of configurations, from boundary layers to plane channels and pipes, attacked both from the experimental and the numerical side, see [2–5] and references therein. Another peculiarity of these phenomena is represented by the non-uniform instantaneous particle configurations at the wall. In fact, particles at the wall seem to accumulate in preferential structures which are extremely long and aligned along the mean velocity direction. The specific nature and dynamics of these structures is still not completely understood, so the aim of our work is to investigate the origin of these phenomena and in particular their link with turbulent large-scale motions.

In the present paper we discuss results from direct numerical simulations of pipe and channel flows to address the effect of the different turbulent large-scale motions on the transport of inertial particles. In a first step, the influence of the flow geometry is considered by comparing turbulent pipe and channel flow. A fully-developed turbulent pipe flow laden with small particles is simulated in a spatially developing configuration. Particles are injected at a fixed location at the axis of the pipe and their evolution is analyzed along a streamwise distance of 200 R (with R the pipe radius). This simulation allows for a better description of the developing stages of the particle accumulation process and it is, moreover, very similar to experimental set-ups. In the far-field, beyond the developing region, we observe a statistically axially-homogeneous particle distribution that presents elongated accumulation patterns. The same phenomenology is then also addressed in a plane geometry, the classical particle-laden turbulent channel flow. This simulation tracks the temporal evolution of a fixed number of particles in the periodic domain. Two cases at the same Reynolds number differing for the domain size were considered to investigate the effects of the periodic boundary conditions on the particle dynamics and accumulation patterns.

2 Methodology and Numerical Methods

2.1 Governing equations

The carrier fluid is assumed to obey the incompressible Navier–Stokes equations,

$$\frac{\partial u_i}{\partial x_i} = 0$$
$$\frac{\partial u_i}{\partial t} + u_j \frac{\partial u_i}{\partial x_j} = -\frac{1}{\rho}\frac{\partial p}{\partial x_i} + \nu \frac{\partial^2 u_i}{\partial x_j \partial x_j}, \tag{1}$$

where u_i is the fluid velocity. The control parameter is the classical Reynolds number, $Re = U_0 L/\nu$, with L either the pipe radius $R_{\max}$ or the channel half-width h and U_0 is an external velocity scale, typically the centerline velocity or the bulk velocity across the section. It is here useful to define the so-called friction Reynolds number $Re_\tau = U_* L/\nu$, where $U_* = \sqrt{\tau_w/\rho}$ is called the friction velocity which is based on the shear stress at the wall τ_w. Quantities with a superscript $+$ are in so-called viscous or inner scaling, i.e. scaled based on U_* and the corresponding viscous length $\ell_\star = \nu/U_*$.

For the dispersed phase we consider the following simplifying assumptions: the particles are rigid spheres with diameters much smaller than the viscous scales of the turbulence, they are very diluted, with density of the solid phase much larger than the fluid one, $\rho_p/\rho = 1000$. Under these conditions the feedback acting on the fluid phase and collisions can safely be neglected (one-way coupling) and the only force acting on the particles is the viscous Stokes drag [6]. The particle dynamics is described by a Lagrangian formulation and each particle evolves according to [7]

$$\frac{\mathrm{d}v_i}{\mathrm{d}t} = \frac{u_i(x_i) - v_i}{\tau_p} \tag{2}$$

$$\frac{\mathrm{d}x_i}{\mathrm{d}t} = v_i, \tag{3}$$

where v_i denotes the particle velocity. This leaves the Stokes number, ratio of τ_p and the characteristic time scale of the carrier fluid, as the only parameter defining the particle dynamics for given flow field. In wall-bounded flows the viscous time ν/U_*^2 is the natural choice, leading to $St^+ = \tau_p {U_*}^2/\nu$. The outer-scale Stokes number is then $St = \tau_p L/U_0 = St^+ Re_\tau^2/Re$. Elastic collisions are assumed when the particle surface hits the wall i.e. when the distance from the particle center to the wall equals the radius. The nominal particle diameter has then an active role in the interaction with the wall, i.e. d_p is an additional dimensionless parameter of the system.

2.2 Pipe flow

For the pipe simulation, the algorithm solves Eq. 1 in cylindrical coordinates with a conservative second order finite difference scheme on a staggered grid. The time evolution is performed by an explicit third order low-storage Runge–Kutta scheme. The base pipe element has the length $L_z = 2\pi R$ and is discretized by a uniform grid of $128 \times 80 \times 128$ nodes in the axial z, radial r and azimuthal θ directions,

respectively. Peak values of turbulence intensities and their locations agree well with the available literature data, see Ref. [3].

The same three-stage third order low storage Runge–Kutta method used for the fluid phase evolves particles positions and velocities according to Eqs. 2 and 3. The interpolation of the fluid velocity $\mathbf{u}$ at the particle position is carried out by a mixed linear-quadratic formula based on Lagrange polynomials. The simulations we describe involve seven different populations of particles ($St^+ = 0.1$, 0.5, 1, 5, 10, 50, 100). For the particle phase the simulation is a spatially evolving one in which the particles are injected near the axis at inlet section with fixed injection rate. The particle evolution is considered in a very long domain that consists of 32 replications of the basic periodic pipe flow element. Being transported by the fluid, particles eventually leave the long domain with no back reaction on the input rate. More details on the simulation setup and tests are given in Ref. [3].

2.3 Channel flow

The simulations in the channel-flow geometry were performed using an adapted version of the general spectral Navier–Stokes solver SIMSON [8]. The wall-parallel directions are discretized with Fourier series, whereas the wall-normal direction is expanded with Chebyshev polynomials; the boundary conditions are thus periodic in the streamwise and spanwise directions, and no-slip at the two walls. The location of the grid points in the wall-normal direction is non-equidistant according to the Gauss–Lobatto distribution. The flow is driven by constant mass flux by adjusting the pressure gradient in each time step. The temporal discretization is achieved via a standard low-storage mixed Runge–Kutta/Crank–Nicolson scheme of third order in which the convective terms are treated explicitly in physical space employing FFT; dealiasing using the 3/2-rule is employed in the wall-parallel directions. The validation of the code for single-phase turbulent channel flow at Reynolds numbers up to $Re_\tau = 590$ yields essentially identical results as the ones published by Moser et al. [9], and are therefore not shown. The code is parallelized using MPI over the spanwise direction, and can therefore be used efficiently on cluster computers.

The integration of the location and velocities of the Lagrangian particles is done in an explicit fashion using the same Runge–Kutta scheme as for the convective terms. The fluid velocities at the particle positions are interpolated using a tri-linear scheme. In particular in the near-wall region the grid spacing due to the Gauss–Lobatto distribution is very fine, such that it is believed that sufficient accuracy can be obtained via the linear interpolation. We remark that a similar interpolation formula was successfully tested and employed in a homogeneous pseudo-spectral DNS [10]. The particle-tracking algorithm is parallelized using MPI as well, thus enabling the treatment of large domains employing on the order of 100 processors.

The code, described in the previous paragraph, has been extensively validated by comparing simulations of particle laden channel flows with available data in literature.

In the channel geometry, we are considering two different simulation domains. The smaller domain is of size $4\pi \times 2 \times 4\pi/3$, which corresponds to a box similar to that of the reference simulation by Kim et al. [11]. A total of $128 \times 129 \times 128$ modes are employed in spectral space. In order to study the effect of limiting box size, we have also studied a substantially larger domain with effective size $12\pi \times 2 \times 4\pi$,

similar to Ref. [12]; the number of grid points is increased accordingly by a factor of 3 in both the streamwise and spanwise directions. For both domain sizes, the same Reynolds number $Re_\tau = 180$ is considered, maintained by a fixed mass flux $Re_b = 2800$. The mesh spacing in the wall normal direction is small enough to resolve the dissipative scales of the flow ($\Delta y^+ = 0.054 \div 4.42$). A total of five populations of inertial particles ($St^+ = 0.2, 1, 5, 10, 50$) and one of tracers are considered, every run evolves 200,000 and 1,800,000 particles per population respectively, in order to keep equal the mean concentration inside the box domain. Actually, the limit of tracers is recovered by inertial particles with vanishing Stokes number so that the particle dynamical Eq. 2 reduces to $v_i = u_i$. Hereafter we denote tracers conventionally by $St^+ = 0$. We remark that the second simulation is performed in the largest domain among those we have found in literature for multiphase flow. The simulations are started from fully developed turbulent velocity fields obtained in the respective boxes. The particules are initially distributed randomly in the whole domain.

3 Results

Simulation results pertaining to the spatially evolving turbulent pipe flow are presented first. A typical instantaneous visualization of the particle locations ($St^+ = 10$) is provided in the top panel of Fig. 1. Note that this figure is not to scale. Particles are injected into the domain near the center axis with fixed input rate. First, the particles are subjected to dispersion by the turbulent fluctuations. In consequence, the particle concentration is getting more uniform across the pipe, and eventually the particles accumulate near the wall. Further downstream of the input section a mean statistical distribution is achieved along the axial direction.

In the bottom panels of Fig. 1, enlargements of the previous visualization are shown for both the region close to the particle inlet (near field, left panel) and

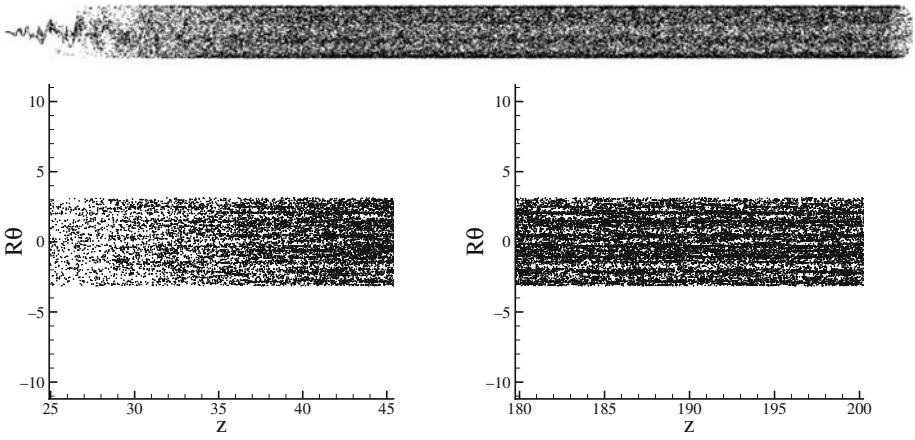

Fig. 1 Instantaneous particle visualization ($St^+ = 10$) in the pipe flow simulation. In the *top panel* a view of the whole computational domain is plotted with arbitrary aspect ratio; *bottom panels* are enlargements of the near field region ($25R < z < 45R$) and far field one ($180R < z < 200R$) respectively along the azimuthal direction in the viscous region

the downstream region (far field, right panel). In the figure the instantaneous particle distribution near the wall is shown after unrolling the pipe along the angular direction. At the beginning of the dispersion process particles tend to accumulate at the wall almost homogeneously both in axial and azimuthal directions displaying some nuclei of particle streaks at the end of the near field region, $z \simeq 40R$. This behavior is consistent with Ref. [3] where it is found that during the transient phase particles tend to sample uniformly the fluid events. Hence particles move towards the wall without having preferential localization or correlation to certain fluid events. However, after reaching statistical stationarity in the axial direction, particles tend to persist in preferential zones organized in long streaky patterns, and the homogeneous wall distribution is lost during this phase. The localization of particles in these patterns is associated with slow fluid departing motions. This feature, enhancing the particle migration from the wall, may balance the turbophoretic drift and may lead to equilibrium conditions, i.e. zero particle wall normal flux. This behavior suggests a strong connection between the asymptotic particle accumulation level and the large scale structures of the flow. In the instantaneous visualization provided in Fig. 1, a qualitative impression of this phenomenon is provided. Further details are discussed in Ref. [3].

As opposed to the spatial development of the particle positions in the pipe flow simulations, the channel flow simulations are set up in a temporally developing fashion. This means that the particles evolve in time from an initially uniform towards a statistically steady distribution. At all times the streamwise x and spanwise z directions are homogeneous, and the particle distributions changes as a function of time t.

As expected a similar accumulation behavior is found for both the pipe and channel simulations, although the transient phase corresponds to the first temporal stages of the simulation. It is noteworthy that in the channel the asymptotic state is reached only after long times depending on the Stokes number. To exemplify the development, two different instantaneous particle configurations are shown in Fig. 2 where the left panel represents the transient state ($t^+ = 450$). This state is—in agreement with the pipe results presented above—also characterized by an

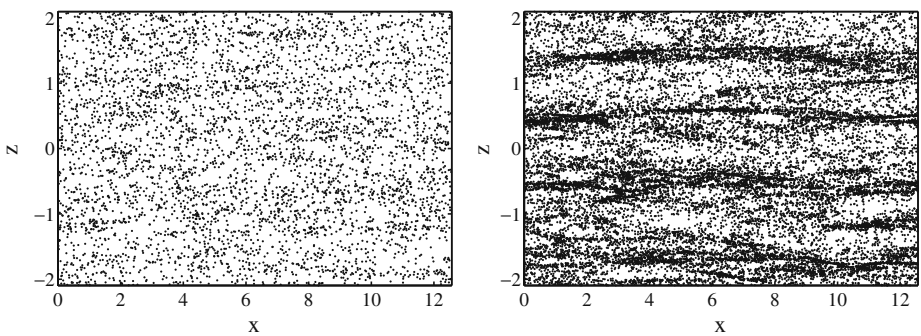

Fig. 2 Instantaneous particle visualization ($St^+ = 10$) in the channel flow simulation (*small box*). *Left* and *right panels* represent a configuration of particles near the wall (viscous) at times $t^+ = 450$ and $t^+ = 17000$ respectively

essentially homogeneous spatial distribution, while a streaky distribution is found for the asymptotic state plotted in the right panel.

The effect of turbophoresis is quantified in Fig. 3 showing the wall-normal profile of the (Eulerian) mean particle concentration C, defined as the number of particles per unit volume. The wall-normal (resp. radial) variation is obtained by employing a finite grid in that direction, and counting the particle number belonging to a certain slice. Actually, this value of C has been normalized with the concentration averaged in the whole section for both pipe (left panel) and channel (right panel) cases. Concentration profiles are characteristics of the asymptotic developed state for both pipe (for long distances downstream) and channel (for long development times). These figures clearly indicate the well-known behavior of particle-laden flows that inertial particles tend to accumulate close to the wall. Fluid tracers, on the

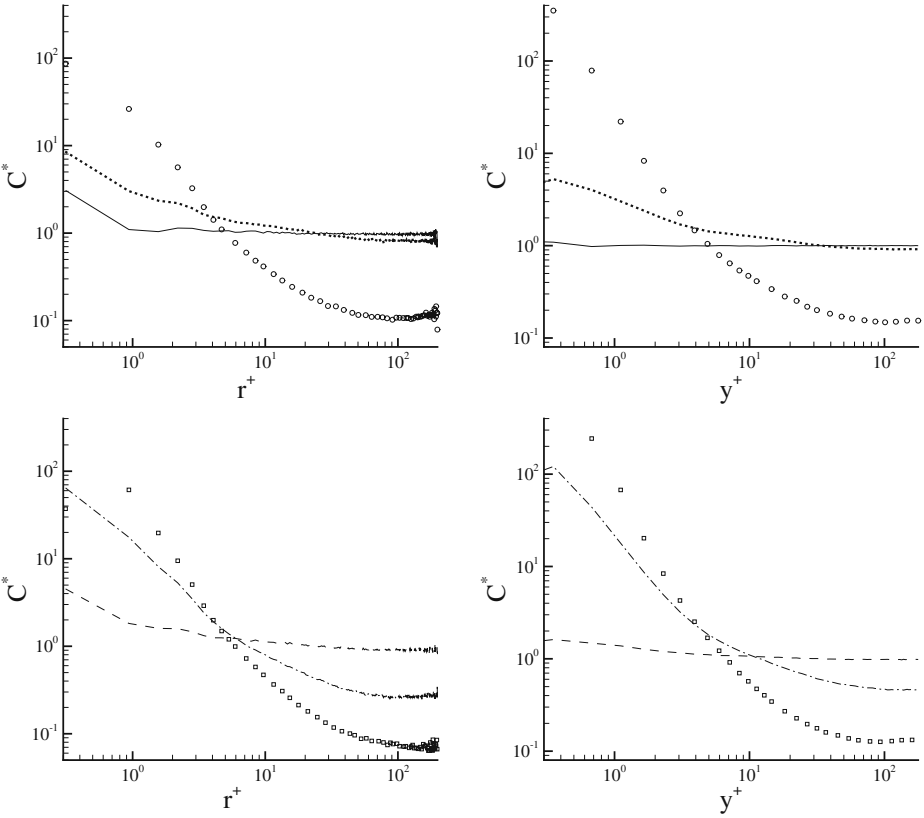

Fig. 3 *Left* and *right panels*: mean normalized concentration c^* (ratio between number of particle per volume and the concentration averaged across the section) of particles in the pipe and channel flow simulation (small domain: (−) $St^+ = 0/0.1$ channel/pipe, (−−) $St^+ = 0.2/0.5$ channel/pipe, (·) $St^+ = 1$, (−·) $St^+ = 5$, (o) $St^+ = 10$, (□) $St^+ = 50$). The binning size is given by the Gauss–Lobatto Eulerian mesh for the channel flow, while a uniform spacing of $\Delta r^+ = 0.625$ is employed for pipe data, in order to keep a similar binning in the viscous region. To avoid clutter particle populations with different Stokes numbers are grouped in two sets represented in *top* and *bottom panels*

other hand, are equally distributed throughout the channel, while most accumulating particles ($St^+ = 10$ and 50) show values of the wall concentration up to thousand times greater than that at the center of the channel. The trend of turbophoresis is similar in both flow configuration although the maximum wall accumulation in channel flow for $St^+ = 10, 50$ is twice that of the pipe.

Motivated by the visual appearance of the particle distribution in the channel geometry (see e.g. Fig. 3), the effect of the finite box size, both in streamwise as well as spanwise directions, might be an important contribution to the final asymptotic state of the particles. We therefore present now an analysis of a larger channel, which was subjected to a similar mean particle load as the smaller channel. Figure 4 reports the differences between small and large domain channel flow simulations in terms of concentrations. In order to evaluate the main effect of the limiting boundary conditions on the accumulation level we introduce the relative error of mean concentration, defined as

$$err(y^+) = \frac{C_L^*(y^+) - C_S^*(y^+)}{C_S^*(y^+)} 100\,, \tag{4}$$

where C_L^* and C_S^* are the mean normalized concentration in the large and small domains, respectively. In the left panel of Fig. 4 the behavior of *err* is shown for particles characterized by a Stokes number of $St^+ = 10$ and 50. Lighter particles appear to be less affected by domain dimensions, and therefore are not shown in the figure. For the heavier particles, the increase of wall accumulation for both populations $St^+ = 10, 50$ in the larger domain becomes apparent, with a 10 percent difference in wall concentration for the heaviest particle family.

In the right panel of Fig. 4, the mean normalized particle concentration in the viscous sublayer is plotted as a function of the simulation time, scaled in viscous units. In particular, the asymptotic developed state is achieved after a very long time of the order of $\sim 10^4$ viscous time scales in accordance with the data of Portela et al. [2] for

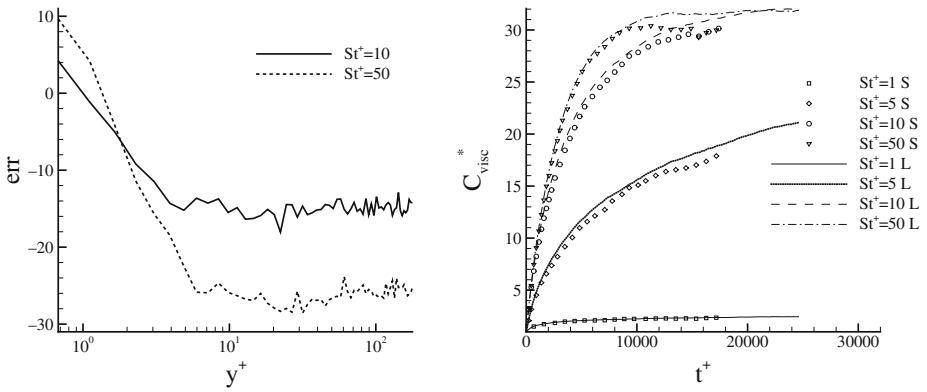

Fig. 4 Channel flow simulations, comparison between the two different domains. *Left panel*: relative error between mean concentrations in large and small domains respectively. *Right panel*: mean normalized concentration C^* in the viscous sublayer. *Symbols* and *lines* are referred to small and large domain, respectively

$St^+ = 25,\ 100$ particles. It should be noted that particles should cross many times a single periodic domain. In particular, the mean time scale that a fluid particle needs to cross a single periodic domain is $T_c^+ \simeq 150$ for the smaller domain and $T_c^+ \simeq 450$ for the larger one. During the transient phase a very good matching between the two simulations can be observed. The main differences arise in the developed state where the viscous concentrations exhibit relevant difference between the small and large domain simulations; in particular for the most massive particles.

Since, the deposition rate is the net number of particles depositing at the wall per unit surface and unit time, this quantity is not a constant, even for a given flow and for given initial conditions for the particles. This is immediately clarified by looking at the right plot of Fig. 4, whose local slopes actually coincides with the respective deposition rates. Clearly equilibrium conditions are reached when the net particle flux towards the wall vanishes. From our results, it is clear that the more the flow approaches the statistical steady state, the larger is the error in the estimate of the instantaneous deposition rate provided by an insufficiently large domain.

Hence the different large scale motions allowed by the two domain sizes do not noticeably affect the transient accumulation phase while they are more felt in the asymptotic regime. We remark that the developed state is dominated by preferential localization of particles in slow departing fluid motions [3, 4] which are controlled by large-scale structures of the flow. Much work has been done on the unladen turbulent channel flow on the effects of the domain truncation on the near wall structures, see among others [12]. For instance, streamwise spectra do change appreciably with domain size and the velocity fluctuations easily happen to be not fully decorrelated across the domain. What is intriguing in this context, is that the effects on the particles are much more evident, taking place already in simple first order observables like the mean concentration. When multiple-point fluid velocity correlations change, the inertial response of the particles leads to a sensibly different collective behavior of the clusters.

Concerning the transient phase, each particle population presents a different characteristic time to achieve a temporal steady state and in particular this time seems to be inversely proportional to inertia (Fig. 4). This behavior is in contrast with the developing length (the length at which the asymptotic regime begins) found in spatial developing simulations of [3], where this length is found to always increase with St^+. In the past, a number of papers tried to estimate this developing length by multiplying the time at which the asymptotic regime is reached with a characteristic velocity such as the bulk velocity. Since in the developing particle-laden pipe, this length is of order $100 \div 150$ pipe radii [3], the characteristic velocity U_c can not coincide with the bulk velocity U_0 (here $U_0 \simeq 15\, U_*$) and it seems to be better correlated with the characteristic velocity of the viscous sub-layer $U_c \simeq U_*$. Nonetheless the contrasting scaling with St^+ found between spatial and temporal evolving simulations advises that it is presumably hard to rescale exactly the temporal evolving behavior to infer characteristic length scales for the spatial developing case.

To investigate in more detail the accumulation structures at the wall we make use of the two-point correlation coefficient of the Eulerian concentration c. In Fig. 5 streamwise $\langle c'(x)c'(x+\Delta x)\rangle_{x,z,t}(y)$ and spanwise two-point correlations $\langle c'(z)c'(z+\Delta z)\rangle_{x,z,t}(y)$ are shown for particles close to the wall ($y^+ = 1$) in the two channel configurations. Concerning the simulation performed in the smaller periodic domain, particles with a small Stokes number are correlated neither in the streamwise nor in the spanwise direction. Actually their two-point correlations decay to zero already

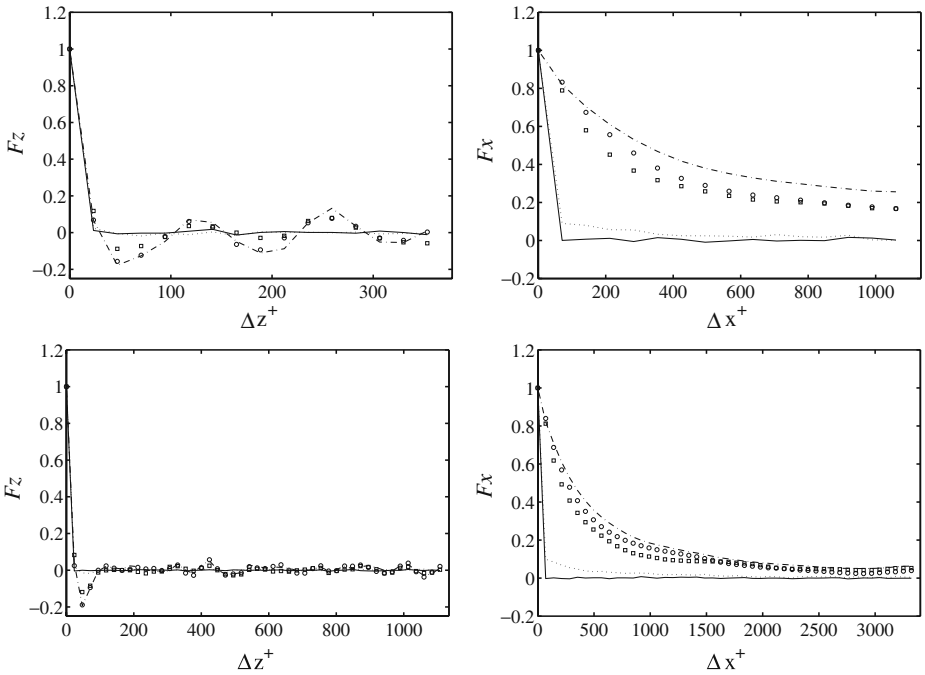

Fig. 5 Spanwise two-point correlation coefficients (*left panels*) and streamwise autocorrelation coefficients of particle concentration fluctuations (*right panels*) (at $y^+ = 1$) obtained in the channel geometry. *Top* (*bottom*) panels are pertaining to the small (large) simulation domain, respectively. The binning size used to evaluate concentrations is $\Delta x^+ = 70$, $\Delta y^+ = 2$, $\Delta z^+ = 24$. Symbols as in Fig. 3

at the smallest separation distance. However, heavier particles are more correlated and in particular a clear sinusoidal behavior is observed in the spanwise direction. The characteristic length of these structures is $\Delta z^+ \approx 120$, featuring a similar spacing as the turbulent velocity streaks measured by spanwise two-point correlation of the streamwise velocity at similar wall distance [11]. However, unlike for the velocity correlations, the particle concentration shows a clear sinusoidal behavior of the two-point correlation even at larger separations, e.g. multiples of the basic separation $\Delta z^+ \approx 2 \cdot 120$. This clearly indicates that the particle patterns are much more regular and straight than the corresponding velocity streaks. The fact that clear maxima and minima appear at e.g. $\Delta z^+ \approx 2 \cdot 120$ shows that the particle streaks are moving in a much more collaborative manner than the velocity.

The simulation results obtained in the larger domain shows a similar negative peak in the spanwise correlation, although the sinusoidal trend for large separations appears clearly attenuated. It is therefore apparent that the very regular and temporally invariant accumulation pattern characteristic for the smaller boxes is to a certain extent due to the restricting boundary conditions. In the larger domain the particle clusters are presumably much more affected by the direct action of the underlying velocity fluctuations, whereas in the smaller domain these motions were

inhibited by the small box. In addition, it is interesting to note that the actual value of the first minimum is unchanged between the small and large simulation domain. This indicates that the localization for a single streak is independent of the periodic boundary conditions, but rather the collective behavior is influenced by them.

As far as the streamwise correlations are concerned, the lightest particles show again no significant spatial correlation in neither simulation domain. For $St^+ > 5$ the long structures visible in Fig. 2 give rise to positive correlations even for large streamwise displacement, certainly not reaching zero (i.e. streamwise independence) in the case of the smaller domain. This is further highlighted by the fact that the actual values computed for the large box for the streamwise correlation at fixed separation are lower than for the small box. As an example, for $St^+ = 5$ at $\Delta x^+ = 1000$, a value of ~ 0.35 is computed in the small box simulation, while the value of ~ 0.2 emerges from the large domain DNS. This results clearly show that particle streaks extend for very long distances and are influenced by the periodic boundary conditions if a typical domain extension suited for monophase DNS is considered.

Similar plots for the two-point correlations in the pipe flow have been computed and are presented in Fig. 6. In the left panel spanwise correlation is shown; also for the pipe flow a clear sinusoidal behavior is observed, although the characteristic width of particle patterns is measured as $r^+\Delta\theta \approx 160$ and seems thus to be greater than that of the channel. Actually for the pipe flow simulation, the spacing of the velocity streaks is $r^+\Delta\theta \approx 120$ that is slightly larger compared to the channel flow. Note that the periodicity in the azimuthal direction is of course due to the pipe geometry, and therefore not artificially imposed.

The streamwise correlation is characterized by a behavior very close to that of channel flow with a major exception of the particles with $St^+ = 5$ which appear to be much less correlated in the streamwise direction as compared to the channel. The differences found mainly in the streamwise correlation, may be attributed more to the spatial developing versus time evolving configurations in respect to differences between pipe and channel geometries.

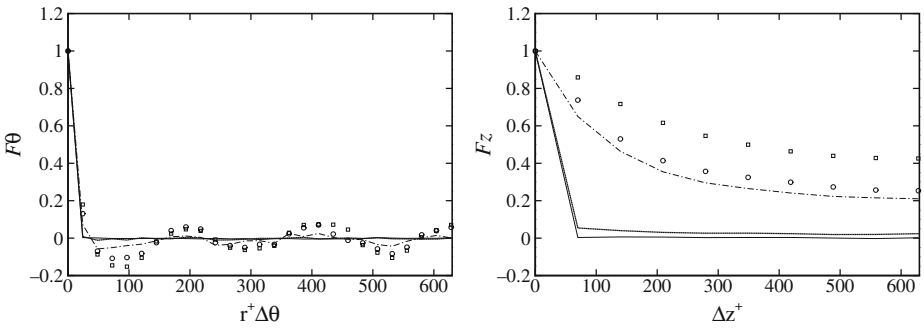

Fig. 6 Spanwise two-point correlation coefficient (*left panel*) and streamwise autocorrelation coefficient of particle concentration fluctuations (*right panel*) (at $y^+ = 1$) of pipe flow simulation. The binning size used to evaluate concentrations is $\Delta z^+ = 70$, $\Delta r^+ = 2$, $r^+\Delta\theta = 24$. Symbols as in Fig. 3

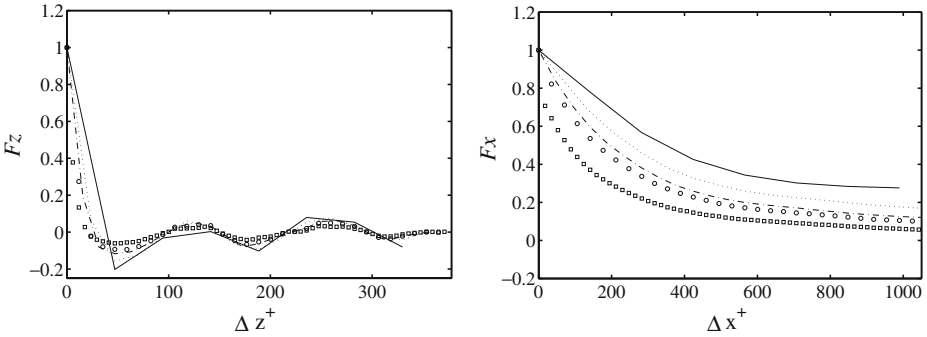

Fig. 7 Spanwise two-point correlation coefficient (*left panel*) and streamwise autocorrelation coefficient of particle ($St^+ = 10$) concentration fluctuations (*right panel*) at ($y^+ = 1$) at varying concentration binning dimensions, symbols: Δx^+, Δy^+, Δz^+, (−) 140, 2, 48, (·) 70, 2, 24, (−·) 47, 2, 16, (*o*) 35, 2, 12, (□) 17.5, 2, 6

We remark that the local particle concentration necessary to evaluate the previous Eulerian statistics depends on the adopted volume size. The effect of the binning for these statistics is quantitatively assessed in Fig. 7 where spanwise and streamwise particle concentration correlations are plotted as a function of the binning size for particle family with $St^+ = 10$. For the spanwise direction, the effect of the binning is mainly given in a more smooth behavior for finer bins, but the spanwise separations of the various maxima and minima appears to be independent of the adopted bin size, even when varied by a factor of 8×8.

The two-point correlation in the streamwise direction is more dependent on the choice of the bin size. The higher correlations for larger bins might be explained by the effect of meandering of the structures for long streamwise distances. However, the general conclusion of a comparably strong correlation in the streamwise direction remains true independent of the bin size.

The apparent lack of convergence of the statistical results with reducing bin dimensions is a significant physical effect induced by particle clustering. From theoretical considerations and numerical simulations in homogeneous turbulent flows, it is now reasonably well understood that particle distributions tend to have a singular nature. The extreme bin sensitivity of the statistics should be interpreted from that perspective: particle distributions have (multi)-fractal properties. Binning, depending on bin size, samples a coarse grained version of the actual particle distribution, hence its behavior at a given scale. Actually, for future analysis of Lagrangian data without the effect of binning, new Lagrangian universal observables are needed [13]. Nonetheless by using a specified volume size (equal in inner units) it is still possible to compare the behavior of particles in different flow configurations.

4 Conclusions and Outlook

Simulations of internal turbulent flows with inertial particles have been performed. Pipe and channel configurations are considered to address the effects of the large-scale geometry on the particle accumulation. We consider two simulations in plane

channel geometry with largely different domains to study the effect of periodicity on the particle accumulation characteristics. The smaller box corresponds to a domain already used by Kim et al. [11], whereas the larger domain is 3×3-times larger in the wall-parallel directions. In the channel, the particle population evolves temporally from an initially uniform distribution. In the pipe flow simulation, spatially developing features are analyzed. The Reynolds number for the channel simulations is $Re_\tau = 180$ and for the pipe flow $Re_\tau = 200$.

In an initial phase after starting either the temporally evolving channel of the spatially evolving pipe flow, the particles show an almost uniform distribution across the flow domain. In the channel, the development time (i.e. the time until stationarity of the particle distribution is reached) is seen to scale inversely with the inertia; this development time seems largely unaffected of the domain size, however.

Turbophoresis occurs among all the cases considered and it is most effective for particles with $St^+ = 10 \div 50$, although differences in the level of asymptotic wall accumulation are found among the configurations. In particular, concerning most accumulating particles, the particle concentration close to the wall is increased by 10% for the larger domain compared to the smaller one. Additionally, it is shown that the wall accumulation for the pipe is only about half that of the channel.

Particles in the developed state predominantly form narrow, but very long streamwise patterns, located preferably along low-speed streaks [3, 4], characterized by an outward wall-normal motion. However, the analysis of the streamwise two-point correlations clearly shows that the length of these particle streaks is significantly larger than the corresponding velocity structures in both channel and pipe. In particular, it is shown that for the smaller channel box, a box similar to what has been commonly used in other studies, the spanwise organization of the particle streaks is extremely regular and corresponds to a mean spacing of about 120 (in pipe a spacing of 160 viscous units is observed); the streamwise two-point correlation of the particle concentration does not go to zero at the ends of the domain. This clearly indicates that such a domain is not large enough for the particles to freely move about.

As discussed in the text, the level of near-wall particle concentration depends on the dynamics of the large-scale patterns which are preferentially located in correspondence to slow outward fluid events. The differences in the accumulation level, found between large and small domain simulations, is attributed to the different behavior of the large-scale patterns as documented by distinct correlations of particle concentration. A possible explanation of this feature can be related to large-scale structures of velocity field, which might carry a considerable amount of energy (see e.g. [12]). These structures usually scale in outer units (in channel flow with the half-height h), and span the whole vertical extent. The influence of these structures on the particle pattern has not been studied before and probably is the key to understand the particle pattern formations.

The last remarks concerns the binning size effects on Eulerian statistics. The correlation of the concentration here adopted to characterize the large-scale accumulation patterns are found sensitive to the binning size. In particular increasing the Eulerian volume size the values of the correlation coefficients appear amplified. In the present work we carefully chose the same volume size (in inner units) to allows a significant comparison among the considered cases. Nonetheless, the need of Lagrangian statistics, which do not depend on the binning size, appears evident to produce universal observables.

References

1. Reeks, M.W.: The transport of discrete particles in inhomogeneous turbulence. J. Aerosol Sci. **14**(6), 729–739 (1983)
2. Portela, L.M., Cota, P., Oliemans, R.V.A.: Numerical study of the near-wall behaviour of particles in turbulent pipe flows. Powder Technol. **125**(2), 149–157 (2002)
3. Picano, F., Sardina, G., Casciola, C.M.: Spatial development of particle-laden turbulent pipe flow. Phys. Fluids **21**(9), 3305 (2009)
4. Picciotto, M., Marchioli, C., Soldati, A.: Characterization of near-wall accumulation regions for inertial particles in turbulent boundary layers. Phys. Fluids **17**, 098101 (2005)
5. Kaftori, D., Hetsroni, G., Banerjee, S.: Particle behavior in the turbulent boundary layer. I. Motion, deposition, and entrainment. Phys. Fluids **7**(5), 1095–1106 (1995)
6. Armenio, V., Fiorotto, V.: The importance of the forces acting on particles in turbulent flows. Phys. Fluids **13**, 2437 (2001)
7. Maxey, M.R., Riley, J.J.: Equation of motion for a small rigid sphere in a nonuniform flow. Phys. Fluids **26**, 883 (1983)
8. Chevalier, M., Schlatter, P., Lundbladh, A., Henningson, D.S.: SIMSON: A Pseudo-spectral Solver for Incompressible Boundary Layer Flows. Mekanik, Kungliga Tekniska högskolan (2007)
9. Moser, R.D., Kim, J., Mansour, N.N.: Direct numerical simulation of turbulent channel flow up to $\mathrm{Re} = 590$. Phys. Fluids **11**, 943 (1999)
10. Gualtieri, P., Picano, F., Casciola, C.M.: Anisotropic clustering of inertial particles in homogeneous shear flow. J. Fluid Mech. **629**, 25–39 (2009)
11. Kim, J., Moin, P., Moser, R.: Turbulence statistics in fully developed channel flow at low Reynolds number. J. Fluid Mech. **177**(1), 133–166 (1987)
12. Del Alamo, J.C., Jimenez, J.: Spectra of the very large anisotropic scales in turbulent channels. Phys. Fluids **15**, L41 (2003)
13. Ijzermans, R.H.A., Reeks, M.W., Meneguz, E., Picciotto, M., Soldati, A.: Measuring segregation of inertial particles in turbulence by a full Lagrangian approach. Phys. Rev. E **80**(1), 15302 (2009)